Supplementary Information (SI) for Physical Chemistry Chemical Physics.

Supporting Information

Magnetic field enhanced discharge and water activation of atmospheric pressure plasma jet: effect of assistance region and underlying physico-chemical mechanism

Xiong-Feng Zhou [1], Bin Chen [1], Hua Liao [2], Kun Liu [1*]

[1] State Key Laboratory of Power Transmission Equipment Technology, School of Electrical Engineering, Chongqing University, Chongqing 400044, People's Republic of China

[2] Taizhou Power Supply Company, State Grid Zhejiang Electric Power Co., Ltd, Taizhou 31800, People's Republic of China

*Authors to whom correspondence should be addressed: liukun@cqu.edu.cn (Kun Liu)

S1. Selection of magnetic induction intensity

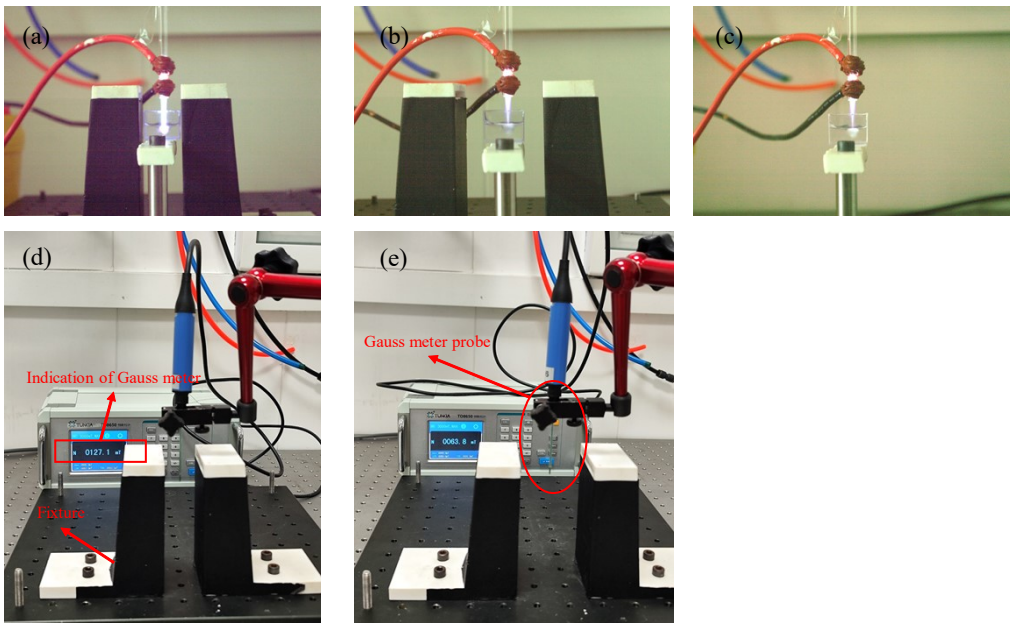

Figure S1 Effects of magnetic induction intensity on discharge: (a) 127.1 mT, (b) approximately 63.8 mT, and (c) 0 mT; and construction of fixture generating different magnetic induction intensities: (e) 127.1 mT, (f) approximately 63.8 mT

Figure S1 shows the effects of magnetic induction intensity on discharge. In figures S1(a) and S1(e), the magnets were positioned just 4 cm apart, resulting in an intensity of approximately 130 mT (127.1 mT) in the discharge space. This was the achievable maximum intensity for experiment. By shifting one fixture by a minimum unit distance (equivalent to the spacing between two holes on the optical table, approximately 2.5 cm) in figures S1(b) and (f), the intensity coincidentally halved to approximately 65 mT (63.8 mT). However, at this reduced intensity, the magnetic field had negligible effects on the discharge whose behaves essentially the same as it would without a magnetic field in figure S1(c). Thus, a magnetic induction intensity of approximately 130 mT was chosen for experiments.

S2. Calculation of physical parameters and •OH number density

S2.1 Typical optical emission spectra (OES)

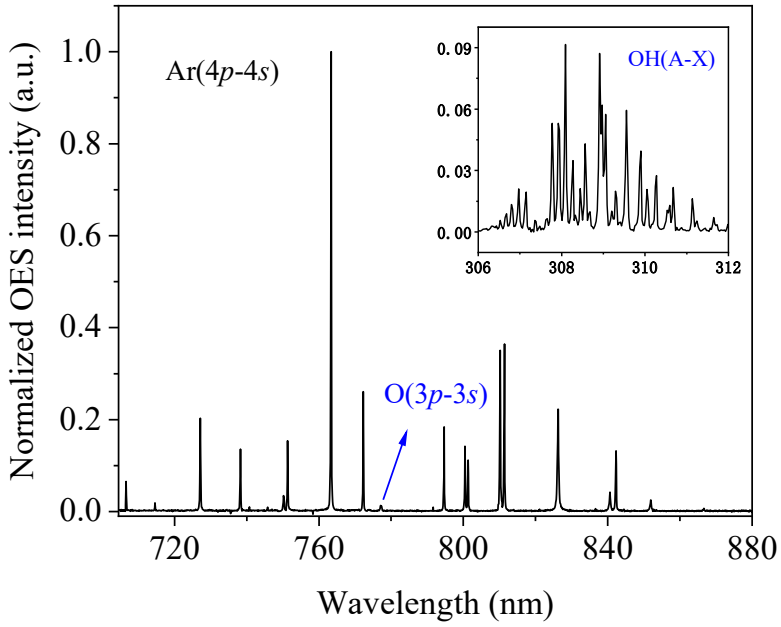

Figure S2 Typical OES of argon-atmosphere plasma jet

S2.2 Gas temperature

Optical emission spectroscopy was a non-intrusive method that was widely used for diagnosing plasma gas temperature. Due to the low collision quenching reaction rate with ambient particles in argon-dominated atmospheric pressure discharge, the effective lifetime of OH(A) species was generally relatively long that exceeding its rotational energy relaxation time. It meat that OH(A)

species undergone sufficient energy exchange with ground-state particles to achieve thermal equilibrium before de-excitation. Therefore, the rotational temperature of OH(A) T_{rot} could be used to represent the gas temperature T_g. Gas temperature T_g was calculated through the Boltzmann slope method as follows:

$$\ln\left(\frac{I_{N'N''}\lambda_{N'N''}}{(2N'+1)A_{N'N''}}\right) = \ln\left(\frac{N_v hc}{Q_{rot}}\right) - \frac{F(N')hc}{K_B T_g} \quad (1)$$

where $I_{N'N''}$ and $\lambda_{N'N''}$ were the spectral line intensity and corresponding wavelength (transition as OH(A-X)), respectively, when electrons transition from a rotational energy level N' on a certain electronic state (OH(A)) to a rotational energy level N'' on another electronic state (OH(X)); $A_{N'N''}$ was the transition probability, N_v was the population of particles on the vibrational state at N' of the upper energy level OH(A), h was Planck's constant, c was the speed of light, Q_{rot} was the rotational partition function, $F(N')$ was the rotational term energy at N' of the upper energy level OH(A), and K_B was Boltzmann's constant.

Figure S3 shows the schematic diagram for calculating gas temperature T_g in the absence of magnetic field, and the selected OH(A-X) line wavelengths and related constants are given in Table S1. It should be noted that since the jet discharge generated a non-thermal equilibrium plasma, the rotational freedom of OH(A) species had not fully reached thermal equilibrium with the ground-state molecules resulting in multiple slopes appearing during the fitting process. Generally, the lower temperature T_1 was chosen to represent the gas temperature T_g.

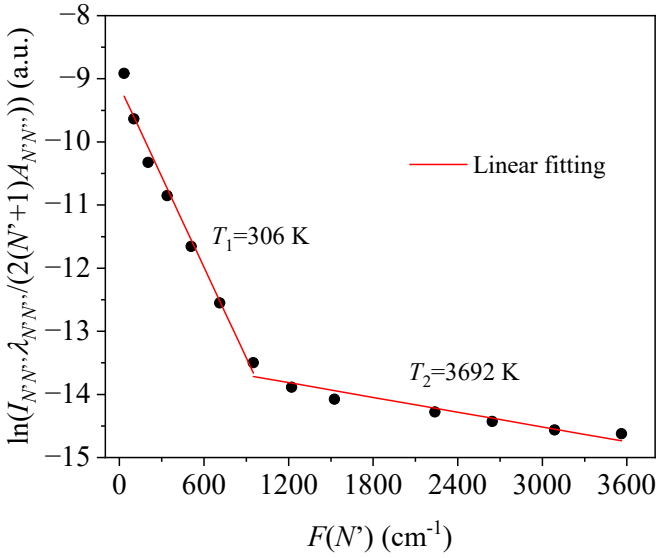

Figure S3 Schematic diagram for calculating gas temperature

Table S1 Selected OH(A-X) line wavelengths and related constants for calculating gas temperature

$\lambda_{N'N''}$ (nm)	N'	$A_{N'N''}$ (s^{-1})	$F(N')$ (cm^{-1})	$\lambda_{N'N''}$ (nm)	N'	$A_{N'N''}$ (s^{-1})	$F(N')$ (cm^{-1})
307.85	1	4.11e+05	33.92	310.92	12	6.06e+05	2645.92
308.00	2	5.16e+05	101.77	311.01	13	5.98e+05	3086.90
308.33	4	6.04e+05	339.22	311.46	14	5.84e+05	3561.81
308.52	5	6.24e+05	508.83	312.37	8	3.77e+05	1221.19
308.73	6	6.35e+05	712.36	313.43	9	3.51e+05	1526.49
309.45	7	6.28e+05	949.82	314.37	11	3.44e+05	2238.852
310.32	3	3.82e+05	203.53				

S2.3 Electron excitation temperature

Abundant Ar(4*p*-4*s*) spectral lines were observed in the optical emission spectra, and these lines could be used to calculate electron excitation temperature T_{exc} through the Boltzmann slope method as follows:

$$\ln\left(\frac{I_{pk}\lambda_{pk}}{g_p A_{pk}}\right) = \ln\left(\frac{N_a hc}{Q_{exc}}\right) - \frac{E_p}{K_B T_{exc}} \tag{2}$$

where I_{pk} and λ_{pk} were the spectral line intensity and corresponding wavelength, respectively, when electrons transition from the high-energy state p to the low-energy state k of the atom; g_p was the statistical weight of the high-energy state, A_{pk} was the transition probability, N_a was the total population of atoms, Q_{exc} was the atomic partition function, and E_p was the energy of the high-energy state. For the same atom, the term of $\ln\left(\frac{N_a hc}{Q_{exc}}\right)$ could be regarded as a constant. Creating a scatter plot of $\ln\left(\frac{I_{pk}\lambda_{pk}}{g_p A_{pk}}\right)$ versus E_p and then obtaining the slope through linear fitting, it allowed to calculated electron

excitation temperature T_{exc}.

Figure S4 shows the schematic diagram for calculating electron excitation temperature T_{exc} in the absence of magnetic field, and the selected Ar(4*p*-4*s*) line wavelengths and related constants are given in Table S2.

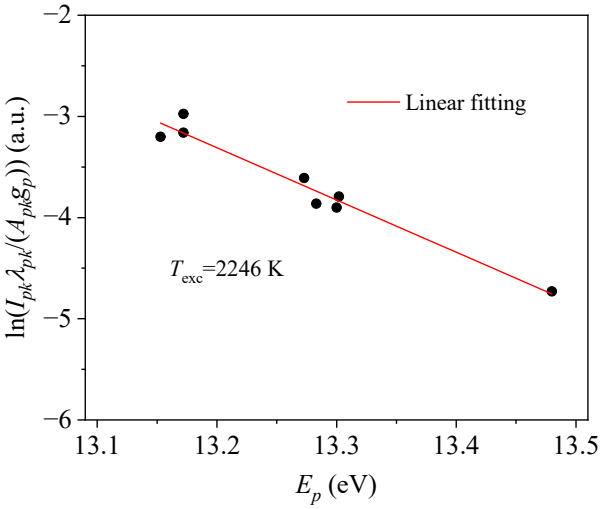

Figure S4 Schematic diagram for calculating electron excitation temperature

Table S2 Selected Ar(4*p*-4*s*) line wavelengths and related constants for calculating electron excitation temperature

λ_{pk} (nm)	g_p	A_{pk} (s^{-1})	E_p (eV)	λ_{pk} (nm)	g_p	A_{pk} (s^{-1})	E_p (eV)
706.72	5	3.80e+06	13.30	763.51	5	2.45e+07	13.17
738.40	5	8.50e+06	13.30	794.82	3	1.86e+07	13.28
750.39	1	4.5e+07	13.48	800.62	5	4.90e+06	13.17
751.47	1	4.00e+07	13.27	810.37	3	2.50e+07	13.15

S2.4 Electron density

The spectral line of argon atom at wavelength λ of 696.54 nm was used to calculate electron density, with the full width at half maximum $^{\Delta\lambda_V}$ of a Voigt profile expressed as follows,

$$\Delta\lambda_V = \sqrt{\Delta\lambda_G^2 + (\frac{\Delta\lambda_L}{2})^2} + \frac{\Delta\lambda_L}{2} \quad (3)$$

where $\Delta\lambda_G$ and $\Delta\lambda_L$ were Gaussian broadening and Lorentzian broadening, respectively, which comprised the following broadening components:

$$\Delta\lambda_G = \sqrt{\Delta\lambda_D^2 + \Delta\lambda_I^2} \tag{4}$$

$$\Delta\lambda_L = \Delta\lambda_{van} + \Delta\lambda_s + \Delta\lambda_R \tag{5}$$

where $\Delta\lambda_D$, $\Delta\lambda_I$, $\Delta\lambda_{van}$, $\Delta\lambda_s$, and $\Delta\lambda_R$ were Doppler broadening, instrumental broadening, van der Waals broadening, Stark broadening, and resonance broadening, respectively. Resonance broadening $\Delta\lambda_R$ could be ignored (on the order of 10^{-5} nm), instrumental broadening $\Delta\lambda_I$ was 0.0720 nm in this case, and other broadenings could be expressed as follows,

$$\Delta\lambda_D = 7.16 \times 10^{-7} \lambda \sqrt{\frac{T_g}{M}} \tag{6}$$

$$\Delta\lambda_{van} = 6.8 \times 10^{-3} \left(\frac{T_g}{296}\right)^{-0.7} \tag{7}$$

$$\Delta\lambda_s = 2 \times [1 + 1.75 \times 10^{-4} \times n_e^{1/4} \alpha \times (1 - 0.068 n_e^{1/6} T_e^{-1/2})] \times 10^{-16} \omega n_e \approx 2 \times 10^{-16} \omega n_e \tag{8}$$

where M was the relative atomic mass, n_e was the electron density; α, T_e, and ω were the ion impact parameter, electron temperature, and electron impact parameter, which could be regarded as constants at atmospheric pressure with values of 0.032, 11600 K, and 0.00537 nm/cm^3, respectively. Therefore, we could first solve for Gaussian broadening $\Delta\lambda_G$ via equation (4), then calculate Lorentz broadening $\Delta\lambda_L$ through full width at half maximum $\Delta\lambda_V$ via equation (3) , and finally derive electron density n_e via equation (8).

Figure S3 shows the schematic diagram of Voigt function fitting for Ar spectral line obtained in the absence of magnetic field, with a following broadening settings: $\Delta\lambda_L$ of 0.0694 nm (comprising $\Delta\lambda_{van}$ of 0.0001 nm and $\Delta\lambda_s$ of 0.0693 nm), and $\Delta\lambda_G$ of 0.0741 nm (comprising $\Delta\lambda_D$ of 0.0021 nm and $\Delta\lambda_I$ of 0.0720 nm). It was evident that the spectral line fitted well and the $\Delta\lambda_s$ could be used to calculate the electron density n_e. In this instance, n_e was calculated to be 6.45×10^{16} cm^{-3} using equation (8).

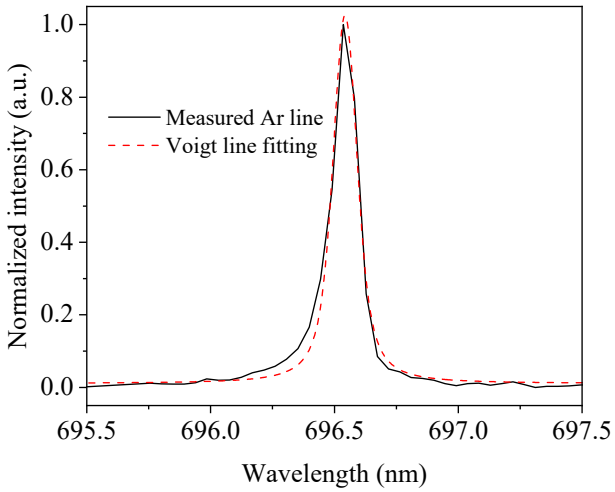

Figure S5 Schematic diagram of Voigt function fitting for Ar spectral line

S2.5 •OH number density

By utilizing the absorption properties of ground state •OH particles (i.e., OH(X)) towards ultraviolet light near 309 nm (transition as OH(X-A)), in-situ absorption spectroscopy measurement was conducted to obtain the absorbance as follows:

$$A(\lambda) = (I_L + I_P - I_{L+P})/I_L = 1 - (I_{L+P} - I_P)/ I_L \quad (9)$$

where $A(\lambda)$ was the absorbance at wavelength λ; I_L, I_P, and I_{L+P} were the spectral intensities under the conditions of UV light on/discharge off, UV light off/discharge on, and UV light source on/discharge on, respectively. Figure S6 shows the schematic diagram for calculating $A(\lambda)$.

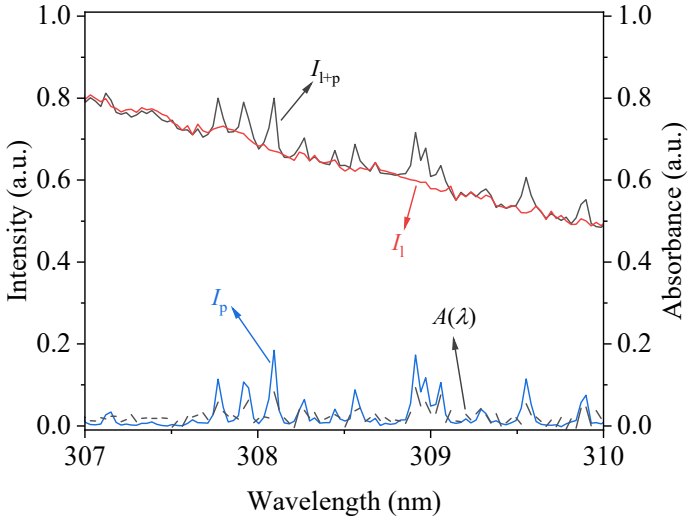

Figure S6 Schematic diagram for calculating absorbance $A(\lambda)$

According to Lambert-Beer's law, the absorbance $A(\lambda)$ could be expressed as follows:

$$A(\lambda) = 1 - \exp(-h\lambda B\varphi(\lambda)n_{N''}L) \tag{10}$$

where B was the absorption coefficients, $n_{N''}$ was the number density of the ground state •OH particles corresponding to the specific rotational energy level N'' at wavelength λ, L was the absorption path length, and $\varphi(\lambda)$ was a normalized linear function as follows,

$$\int \varphi(\lambda)\mathrm{d}\lambda = 1 \tag{11}$$

where the contour of $\varphi(\lambda)$ could be described as a Voigt profile whose explicit function expression as follows,

$$\varphi(\lambda) = \varphi_0 + A\frac{2\ln 2}{\pi^{3/2}}\frac{\Delta\lambda_L}{\Delta\lambda_G^{\,2}}\int_{-\infty}^{+\infty}\frac{\exp(-t^2)}{(\sqrt{\ln 2}\frac{\Delta\lambda_L}{\Delta\lambda_G})^2 + (\sqrt{4\ln 2}\frac{\lambda - \lambda_0}{\Delta\lambda_G} - t)^2}\mathrm{d}t \tag{12}$$

where φ_0 was the offset value, A was the profile area, λ_0 was the center wavelength. Gaussian broadening $\Delta\lambda_G$ (component of $\Delta\lambda_I$ was 0.042 nm in this case) and Lorentzian broadening $\Delta\lambda_L$ could be calculated via equations (4) and (5), and then normalized $\varphi(\lambda)$ was obtained. Finally, by comparing the curve functions on both sides of equation (10), $n_{N''}$ could be derived.

Regarding $n_{N''}$, the number density of ground state •OH particles at a specific rotational energy level N'', it was related the total number density of ground state •OH species n_{tot} as follows:

$$n_{N''} = f_{N''}n_{tot} \tag{13}$$

where $f_{N''}$ was the Boltzmann factor that expressed as follows,

$$f_{N''} = \frac{(2N'' + 1)}{Q_{rot}}\exp(-\frac{F(N'')}{K_B T_g}) \tag{14}$$

where $F(N'')$ was the rotational term energy at the energy level N'' of OH(X). Rotational partition function Q_{rot} was expressed as follows,

$$Q\mathrm{rot} = \sum_{N''}(2N'' + 1)\exp(-\frac{F(N'')}{K_B T_g}) \tag{15}$$

By selecting a spectral line of OH(X-A) ($P_1(2)$ was chosen in our study, with a central wavelength of 308.63 nm, a absorption coefficients B of 2.278×10^9 m^2 J^{-1} s^{-1}, N'' of 2, and $F(N'')$ of 83.8 cm^{-1})

and utilizing the aforementioned formulas, the total number density of ground state •OH species could be calculated based on the absorbance $A(\lambda)$.

S3. Effects of magnetic field on morphology in freestream mode

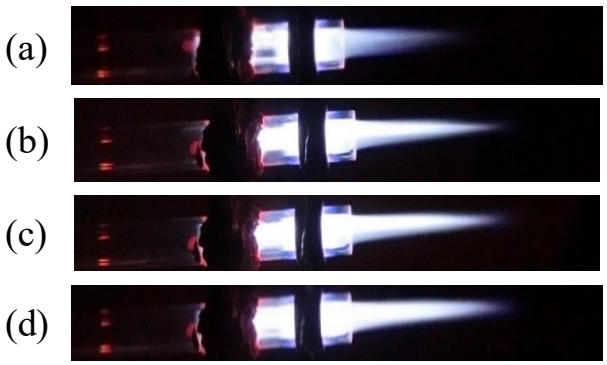

Figure S7 Discharger morphology in freestream mode under different cases: (a) no magnetic field, (b) magnetic field covering two electrodes and plasma plume, (c) magnetic field covering the low-voltage electrode and plasma plume, and (d) magnetic field covering only the plasma plume